

# On One Approach to Parameters Evaluation of Energy Minimizing Image Restoration Methods

Igor V. Gribkov, Peter P. Koltsov, Nikolay V. Kotovich, Alexander A. Kravchenko,  
Alexander S. KoutsaeV, Andrey S. Osipov, and Alexey V. Zakharov

**Abstract** — We study input parameters of energy methods for image restoration, when a restored image is obtained after minimization of an integral functional. Although such a functional is global, only few pixels in a small neighborhood of any pixel on the initial image can influence on the corresponding pixel on the restored image. Conversely, any pixel on the initial pixel affects some pixels in a neighborhood of the corresponding pixel on the restored image. We call these neighborhoods "influence areas" and propose a technique for their calculation and their visualization on computer screen. The whole testing technique based upon this approach is applied to a couple of known image restoration methods. The parameters of these methods, ensuring their better performance, are found.

**Keywords** — energy minimizing methods, image processing, image restoration, image segmentation, testing.

## I. INTRODUCTION

One of the main tasks in evaluation of image processing algorithms is to estimate the best parameters of the considered algorithm for different applications [1]. In recent years, energy minimizing methods, where the output image is the result of minimization of a certain functional in an integral form, found an application in such areas as image segmentation [2]-[3], [11], [14] and image restoration [4]-[19]. In the present paper, we focus on the energy minimizing restoration methods. Nowadays, many types of such functionals, which are used for the restoration of distorted images, are known (see e. g. [15]-[16] and references thereafter). Similar approaches to the restoration problem are intensively studied in recent publications [22]-[26]. The variety of methods creates the need to select the optimal one for a specific practical task.

One can say that image restoration is a state of art technique for enhancement of image quality, based on a few absolute criteria. Generally this process involves some methods for elimination of distortions, for example, such as noise. But in

practice this cannot be done ideally. However, in some cases, significant improvements can be achieved.

In this paper we restrict ourselves to considering the following properties of energy minimizing methods:

a) to reduce significantly the noise level in the parts of the image where the intensity changes smoothly;

b) to protect from blurring the high contrast intensity changes (in other words, to preserve the boundaries of objects on the processed image).

These properties are essential for practical applications and, therefore, their thorough study is important.

The "influence areas" introduced in the paper is a tool which allows one to find out some important features of image restoration methods. We introduce the testing technique based on the use of influence areas and apply it for testing of two known energy minimizing restoration methods. In particular, we find the values of the methods' parameters ensuring their effective performance.

The paper is organized as follows.

In Section II we formulate the main problem considered in the paper.

In Section III we introduce the two types of "influence areas" (further on, we use this term without quotations) and propose a technique for their calculation.

In Section IV, the formulas of functionals for two energy minimizing restoration methods: PL [14] and GR [8], [11] are given. These methods are studied with the help of the influence areas.

The results of the study are presented in Section V.

Finally, we make the conclusions on the optimal methods' parameters choice for both good noise reduction and good contrast boundaries preservation.

## II. PROBLEM SETTING

Let  $I$  be an initial image and  $u$  be a restored image.  $I(x, y)$  and  $u(x, y)$  are corresponding image functions taking integer values from gray level range  $0...255$ .

In our study we use functionals of the following type:

$$E(u) = w_1 \int_{\Omega} (u - I)^2 + w_2 \int_{\Omega} f(\|\nabla u\|^2), \quad (1)$$

where

$E(u)$  – the energy to be minimized,

Manuscript received

All the authors are with the Russian Academy of Sciences, in Scientific Research Institute for System Analysis (Department of Pattern Recognition and Videographic Information Processing).

P.P.Koltsov, e-mail koltsov@niisi.msk.ru

N.V.Kotovich, e-mail nick@genebee.msu.su

A.A.Kravchenko, e-mail alexk@genebee.msu.su

A.S.KoutsaeV, e-mail koutsaeV@niisi.msk.ru

A.S.Osipov, e-mail osipa68@yahoo.com

A.V.Zakharov, e-mail avz@genebee.msu.su

$\|\nabla u\| = \sqrt{(u_x)^2 + (u_y)^2}$  – the gradient norm,

$f(r) \geq 0$  – this function will be described in Section IV,

$\Omega$  – image area  $256 \times 256$  pixels of size,

$w_1, w_2$  – weights specified for items of the equation (1).

Usually  $w_1 + w_2 = 1$ .

Let  $I(x_0, y_0)$  be intensity of a pixel at the location  $(x_0, y_0)$  on the initial image  $I$  (Fig.1.a). The corresponding pixel on the restored image  $u$  has the intensity  $u(x_0, y_0)$  (Fig.1.b). Starting points for our study were two following observations.

a) It appears reasonable that the value  $I(x_0, y_0)$  exerts the most influence on calculating of the value  $u(x_0, y_0)$  under restoration process. It is possible that the value  $I(x_1, y_1)$  of closely spaced pixel  $(x_1, y_1)$  has some influence on calculating of the value  $u(x_0, y_0)$ . At the same time, it seems highly improbable that a peripheral pixel  $(x_2, y_2)$  (Fig.1.a) can have a measurable influence on the value  $u(x_0, y_0)$ . Indeed, if this were not the case, the restored image  $u$  simply would not be similar to the original image  $I$ .

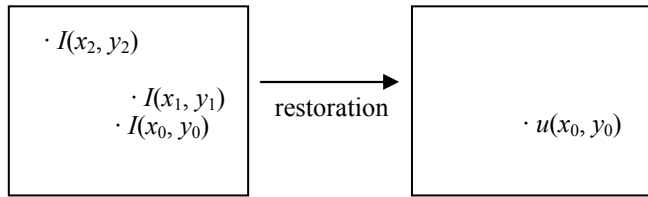


Fig.1.a. Original image

Fig.1.b. Restored image

b) On the other hand, image restoration with functional (1) is a solution of a *global* optimization task: all the pixels of the initial image are used to find  $u(x, y)$ . Hence, the neighboring pixel  $(x_1, y_1)$  and the distant pixel  $(x_2, y_2)$  can formally affect the intensity  $u(x_0, y_0)$  equally.

It appears that items a) and b) contradict one another. So, despite the fact that the functional (1) is global, only some significant pixels located in close proximity to pixel  $(x_0, y_0)$  on the image  $I$ , can have noticeable influence on the value of  $u(x_0, y_0)$ .

The notion of *influence area*, introduced in this paper, is a result of this contradiction. In our view, its determination task comprises the following issues:

1. To find the points on the restored image  $u$  in a certain neighborhood of  $(x_0, y_0)$  affected by intensity change at one pixel  $(x_0, y_0)$  on the initial image  $I$ . Obviously, after the change of intensity value  $I(x_0, y_0)$  and after the restoration of the modified image, not only the value of  $u(x_0, y_0)$  will be changed, but also the intensity values of the pixels near  $(x_0, y_0)$  on the restored image  $u$ . These pixels form a certain neighborhood of  $(x_0, y_0)$  on  $u$  which we call an *influence area of the first kind*.

2. To find the pixels on the initial image  $I$  in a neighborhood of  $(x_0, y_0)$  which affect the intensity change at one pixel  $(x_0, y_0)$  on the restored image  $u$  (their existence is also obvious). We call this neighborhood an *influence area of the second kind*.

Note that to find the influence area of the first kind, one must have the initial image, the restored image, the modification of the initial image and the result of its restoration. Thus the restoration procedure must be done twice. At the same time, in order to find the influence area of the second order, in addition to the initial and the restored image, one must have many modifications of the initial image at one pixel near  $(x_0, y_0)$  and respectively the results of their restorations. Thus, for the calculation of the second order influence area many restorations are needed, which makes the whole process more complicated compared to the first order area calculation.

The goal of our study is to assess the shape and size of such areas. We develop a technique for calculating such areas (Section III) and demonstrate this technique on the example of two known energy minimizing methods (Section IV). For this purpose we use a synthetic image shown on Fig.2. This image is taken from the test image database of our PICASSO system designed for evaluation of various image processing algorithms [15]-[16], [20]-[21].

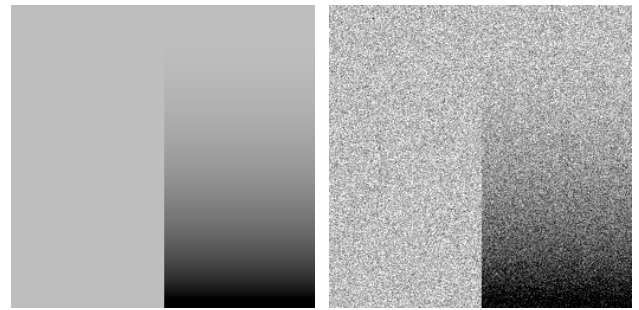


Fig.2.a. Ideal image.

Fig.2.b. Noisy image  $I(x,y)$ .

This image has an inner boundary in the middle. Its contrast varies from bottom to top. Namely, on the Fig.2, the contrast of the boundary pixels is determined by ordinate  $y$  and continuously decreases from the most value at the bottom of the image to the least value at the top. The performance of energy image restoration methods significantly depends on the contrast values near the boundaries [21]. This image allows one to study efficiently the specific features of these methods. It appears that influence areas are significantly different a) if a tested pixel is far from the boundary and b) if it is close to the boundary.

### III. INFLUENCE AREAS AND TECHNIQUE FOR THEIR CALCULATION

We develop the following technique in order to evaluate the size and the shape of influence areas. To do it, the following steps are necessary (1-12):

1. Choose a noisy image having inner boundaries. In this paper we use Fig.2.b. Denote this image as  $I$ .

2. Restore the image using functional (1). Denote the resulting image as  $u$ .

3. Select a pixel  $(x_0, y_0)$  both on  $I$  and  $u$ .

The above three steps are used for calculation of influence areas of both the first and second kind.

The restored image  $u$  is the result of energy functional (1) minimization procedure that includes solving of a differential equation via numerical methods. The solution is usually found by standard iterative process. To do it, all intensity values  $I$  are considered as floating-point values.

The values of restored image  $u$  are also floating-point. Further on, the intensity values of  $u$  are rounded to integers to be displayed on the computer screen.

To calculate the influence areas of the first kind, the following steps are needed (4-6):

4. Modify the image  $I$  in  $(x_0, y_0)$ . Namely, replace  $I(x_0, y_0)$  by  $I_\delta$ , where  $I_\delta(x_0, y_0) = I(x_0, y_0) + \delta$  and  $\delta$  is a small value (see below). In all other points the image  $I_\delta$  is equal to  $I$ .

5. Perform the restoration of  $I_\delta$ . Denote the resulting image as  $u_\delta$ .

6. Find the function  $D_1(x, y) = u_\delta(x, y) - u(x, y)$ .

$D_1(x, y)$  is considered as an image, representing the influence area of the first kind. Formally it has the same size as  $I_\delta$  and  $u_\delta$ . However only a small neighborhood of  $(x_0, y_0)$  contains differences between  $u_\delta$  and  $u$ . Obviously, only this subdomain of  $D_1$  is reasonable to consider.

For the influence areas of the second kind, the corresponding steps (4-6) are different:

4. Perform series of modifications of the image  $I$ : Replace  $I$  with new ones  $I_{\Delta x, \Delta y}(x_0 + \Delta x, y_0 + \Delta y) = I(x_0 + \Delta x, y_0 + \Delta y) + \delta$  where  $\delta$  is a small value, the same for each  $I_{\Delta x, \Delta y}$ . That is, the image  $I$  is changed in a single pixel. In all other points the image  $I_{\Delta x, \Delta y}$  is equal to  $I$ . Values  $\Delta x$  and  $\Delta y$  are sequential integers with step 1. In our experiments we took  $-5 \leq \Delta x, \Delta y \leq 5$ .

The  $\delta$  value should be chosen for the following reasons.

a) Any change of the initial image should not influence essentially the result of restoration. This means that the reduction of  $\delta$  by several times should not considerably change the size, or the shape of the influence area. Our experiments have shown that for  $\delta = 1.0$  and  $\delta = 0.1$  both size and the shape of the influence areas are practically stable. So, such values for  $\delta$  are appropriate. In what follows, the value of  $\delta = 0.1$  is used.

b) For the correct search of distinctions between  $I$  and  $I_{\Delta x, \Delta y}$ , both images should be processed under the same scheme. Since the restored image is found by an iteration method, then in both cases the number of iterations should be the same. For the  $\delta$  choice equal to 0.1, it was observed in all measurements.

5. Perform restorations of all the images  $I_{\Delta x, \Delta y}$ . The restored images will be denoted as  $u_{\Delta x, \Delta y}$ .

6. Find the function  $D_2(\Delta x, \Delta y) = u_{\Delta x, \Delta y}(x_0, y_0) - u(x_0, y_0)$ .

$D_2(\Delta x, \Delta y)$  is considered as an image, and  $\Delta x, \Delta y$  are its coordinates. The values  $\Delta x = 0$  and  $\Delta y = 0$  indicate the center. Intensity value  $D_2(\Delta x, \Delta y)$  shows the influence of change in initial image  $I(x_0 + \Delta x, y_0 + \Delta y)$  on the restoration result  $u(x_0, y_0)$ .

The following steps (7-12) are for better computer screen displaying. They are applied for both  $D_1$  and  $D_2$ , from now on, we denote both functions by  $D$ . Now we make several transformations of the function  $D$  but we keep the same evident notation for it.

7. Cover the function  $D(\Delta x, \Delta y)$  using two-dimensional spline interpolation. Due to this, the coordinates  $\Delta x, \Delta y$  can be treated as floating-point values.

8. Scale the arguments  $\Delta x, \Delta y$  of the function  $D$  so that their range becomes  $0 \dots 127$ . In all subsequent Figs the influence areas are enclosed in squares  $128 \times 128$  pixels of size.

9. Calculate negative image  $255 - D$ . Then the points with the greatest influence on restoration look black, and the points with the least influence look white.

10. Scale the intensity of  $D$  in such a way that its range for non-negative values of  $D$  becomes  $0 \dots 255$ . Negative values of  $D$  (if any) are marked as gray.

11. After scaling of size and intensity, the values of  $D$  have to be rounded to integer. Zero intensity integers outline the borders of the received image  $D$ .

12. Maximum of  $D$  is marked as a center localization pixel.

To calculate an influence area at another pixel  $(x_0, y_0)$ , the steps 1-12 has to be repeated for this pixel. In what follows we consider series of points  $(x_0, y_0)$  located from the left and from the right sides of the inner boundary on Fig.2.

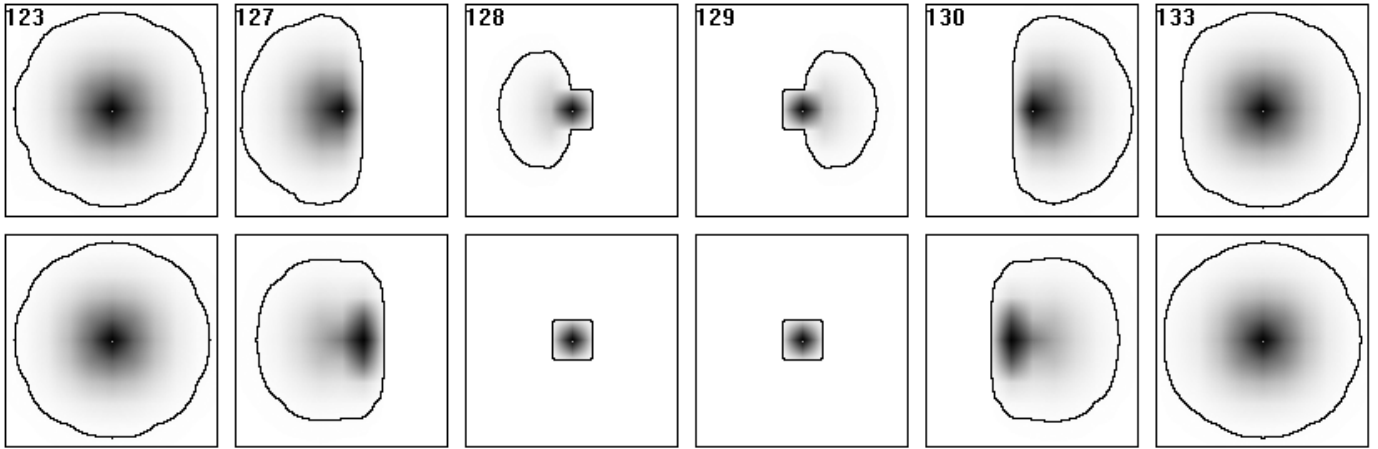


Fig.3. Influence areas calculation example:  $\sigma = 10, y_0 = 27$

On Fig.3 we can see a typical example of influence areas in case when a restoration method “works well”. Some other Figs will be shown in Section V. In all these pictures the first row represents the influence areas of the first kind and the second row the areas of the second kind respectively. Here  $\sigma$  is Gaussian noise deviation, and  $x_0$  accepts values from 123 to 133;  $y_0 = 27$ .

The size of each image on Fig.3 is  $11 \times 11$  pixels; however the images are stretched to the size  $128 \times 128$  pixels by means of splines. The boundary is located between the pixels number 128 and 129 on the horizontal axis of Fig.2. Most interesting is the dynamics of influence areas if tested pixels are approaching to the boundary. One can see that if the pixel (123, 27), (left images on Fig.3), is far enough from the boundary ( $x_0 = 128$ ), both influence area of the first and the second kind are large. While approaching to the boundary, influence areas deform and decrease.

Thanks to this fact the image is blurred in the image areas with no boundaries, so the noise is reduced. But in image areas with boundaries there is no blurring and contrast boundaries are preserved.

#### IV. ENERGY FUNCTIONALS FOR TESTING

Now we apply the technique from the Section III for testing two functionals of type (1). We will keep the notations PL and GR both for functionals and for corresponding image restoration methods.

- 1) PL: functional with Piecewise Linear energy minimizing function, [14];
- 2) GR: modified Geman-Reynolds functional, [8], [11].

Rewrite the formula (1) as

$$E(u) = (1 - \lambda) \int_{\Omega} (u - I)^2 + \lambda \int_{\Omega} c^2 \varphi \left( \left( \frac{\|\nabla u\|}{c} \right)^2 \right), \quad (2)$$

where

$$c^2 = \mu^2 \max_{(x,y) \in \Omega} \|\nabla u(x,y)\|^2, \text{ and } 0 \leq \varphi(r) \leq 1.$$

Here  $0 < \lambda < 1$ , and  $0 < \mu \leq 1$  are two parameters of the functional (2). The parameter  $\lambda$  regulates relative contributions of two terms in the right hand side of (2). Small values of  $\lambda$  restrict a solution to be close to the initial image. Large  $\lambda$  force the solution  $u$  to be smooth. The parameter  $\mu$  controls the properties of the restoration term. The smaller is the value of  $\mu$ , the better is edge preserving qualities and the worse is noise reduction (see below, Fig.4).

The value  $c$  is chosen for proper calculations. Due to such a form of  $c$ , both integral terms in (2) have approximately the same order respective to change of the contrast of the image  $I$ .

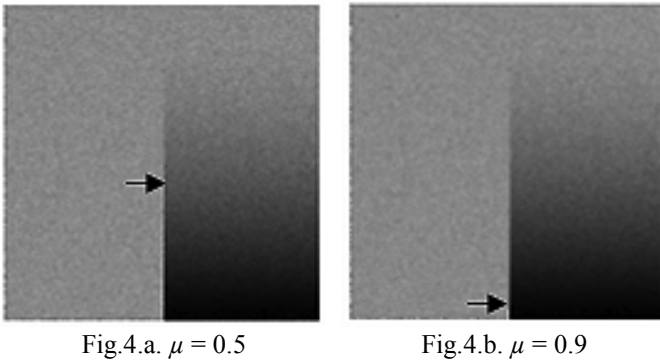
*PL functional.* In [14]-[16], [21] the functionals of type (2) with piecewise linear function (3) were studied:

$$\varphi(r) = r, \text{ if } 0 \leq r \leq 1, \text{ and } \varphi(r) = 1, \text{ if } r > 1. \quad (3)$$

*GR functional.* Primarily, D.Geman and G.Reynolds worked out their functional [8] for image restoration and simultaneous boundary extraction. In [11] this functional was modified for the task of image restoration only. It obtained the form (2) with minimization function (4):

$$\varphi(r) = r/(1+r). \quad (4)$$

The value  $r$  depends on the gradient (2). Functions (3), (4) increase rapidly with  $r$  when the gradient and  $r$  are small on noisy areas with slowly varying intensity. Due to minimization, both gradient term in (2) and gradient are effectively restricted on such areas what results in smoothing of the image  $u$ . Contrarily, the functions  $\varphi$  are constant or increase slowly if the gradient and  $r$  are large near boundaries. In this case, the gradient is less restricted what results in preserving of contrast boundaries.

Fig.4.a.  $\mu = 0.5$ Fig.4.b.  $\mu = 0.9$ 

On Fig.4, we show two images restored using PL method. Here  $\lambda = 0.8$ . If  $\mu = 0.2...0.7$ , the boundaries are well preserved (Fig.4.a), but the noise reduction is bad. If  $\mu = 0.8...0.9$ , noise reduction is better. However, only most contrast boundaries are preserved on the restored image (Fig.4.b). Black arrows on Fig.4 indicate boundary points with critical contrast values. If the boundary's contrast is greater than critical then such a boundary remains contrast after the restoration procedure. If not, the boundary is blurred. We will show that the technique of influence areas allows one to find critical contrast values.

## V. TESTING RESULTS

Minimization problem (2) can be solved by standard iteration method (see e. g. [11]). Our experiments have shown that the parameter  $\lambda$  mainly affects the speed of convergence of the iteration process. For both methods, we obtained good

convergence with  $\lambda=0.8$  to  $\lambda=0.9$ . So, further we use such values of  $\lambda$ . As to the parameter  $\mu$ , it varies within the range  $0 < \mu \leq 1$ . The result of calculations  $u$  very significantly depends on the value of  $\mu$ .

Next we give some examples of influence areas for PL and GR functionals. In all cases, we chose noisy image Fig.1.b with Gaussian noise deviation  $\sigma = 10$ . We tried other values of  $\sigma$ . The results were not quite the same, but similar.

*PL method.* Fig.3 corresponds to PL method at  $\lambda = 0.9$ ,  $\mu = 0.3$ ,  $\sigma = 10$ ,  $y_0 = 27$ . Such influence areas are typical for the values  $\lambda = 0.8...0.9$ ,  $\mu = 0.2...0.8$ .

The restored image is obtained as a solution of a nonlinear differential equation, so influence areas are not always as good as on Fig.3. The situations when a restoration method fails maybe are most informative. On Fig.5 we show influence areas for  $\mu = 0.1$ . One can see gray homogenous domains outside the neighborhood of  $(x_0, y_0)$  in the second row. Within such domains, the function  $D$  is less than zero. It means that small gain of the intensity near the pixel  $(x_0, y_0)$  on the initial image  $I$  does not results in the gain of intensity at  $(x_0, y_0)$  on the restored image  $u$ . Conversely, the intensity at  $(x_0, y_0)$  on  $u$  decreases. Thus, PL method makes certain distortion of the boundary on  $u$ , and for this value of  $\mu$  proves to be "bad".

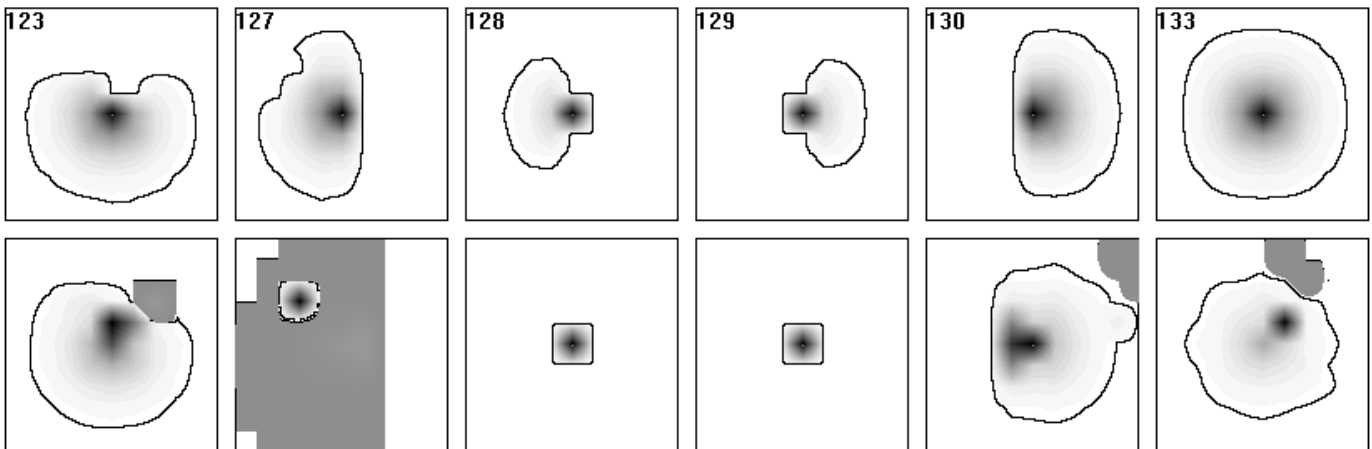
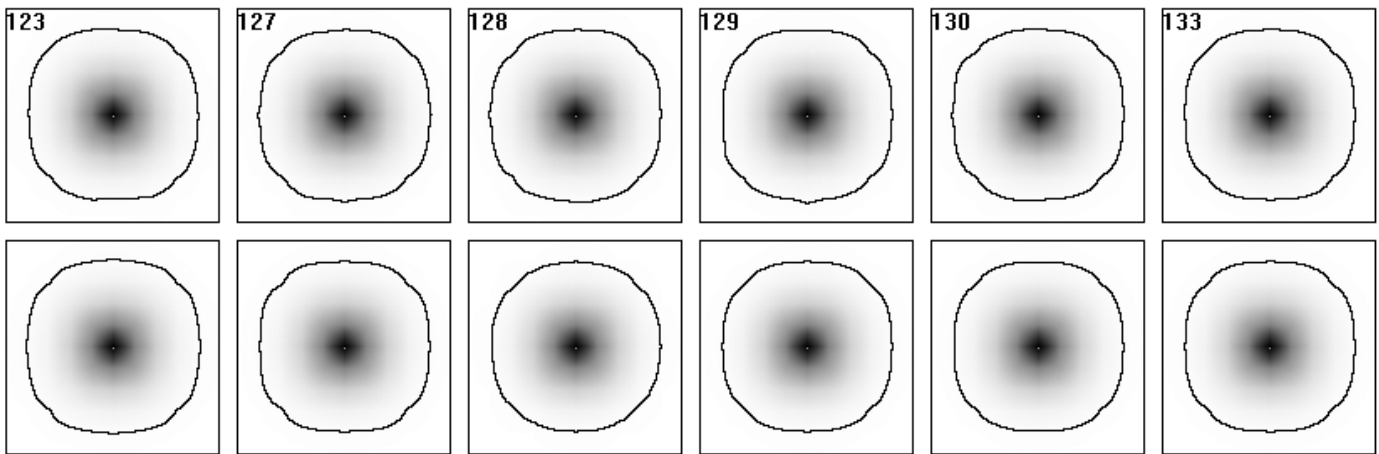


Fig.5. PL method.  $\lambda = 0.8$ .  $\mu = 0.1$ .  $y_0 = 26$ . "Bad" domains in the second row.

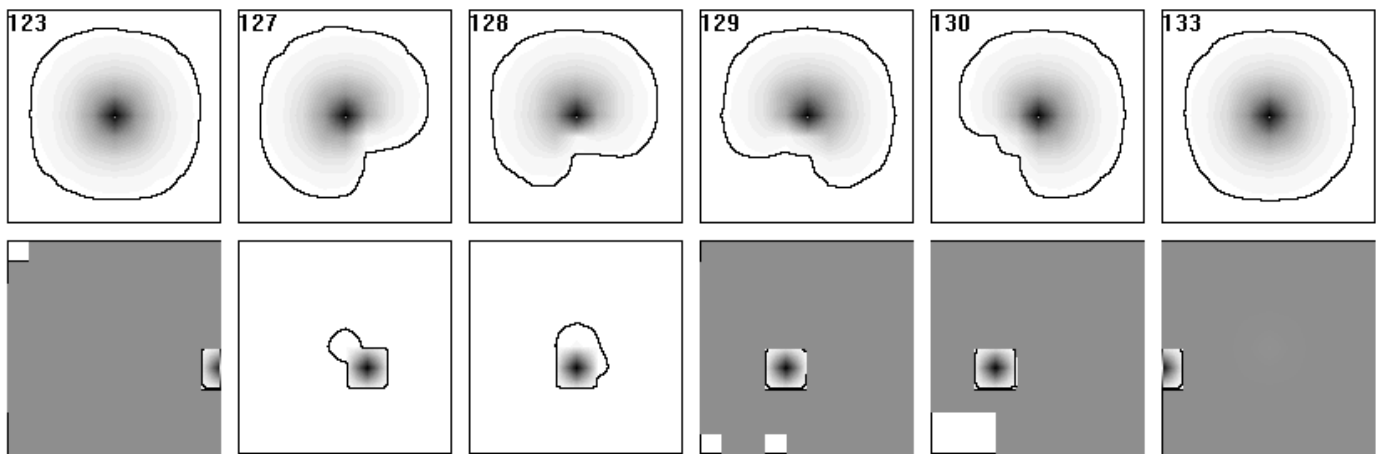
Next let us consider Fig.6. If  $y_0 = 27$ , such a value of  $y_0$  defines too low contrast of the boundary for the given value  $\mu = 0.8$  (see Fig.4). Thus the initial image is blurred around all

points  $(x_0, y_0)$  we test, and the boundary is not preserved at all. On Fig.6 we can see large influence areas both of the first and the second kind. This effect means blurring.

Fig.6. PL method.  $\lambda = 0.8$ .  $\mu = 0.8$ .  $y_0 = 27$ 

Now let us consider Fig.7. The ordinate  $y_0 = 27$  defines critical level of the boundary contrast for  $\mu = 0.7$ . If  $y_0 < 27$ , then more contrast boundary is preserved; if  $y_0 > 27$ , it is not (Fig.4). As is seen on Fig.7, the shape of influence areas

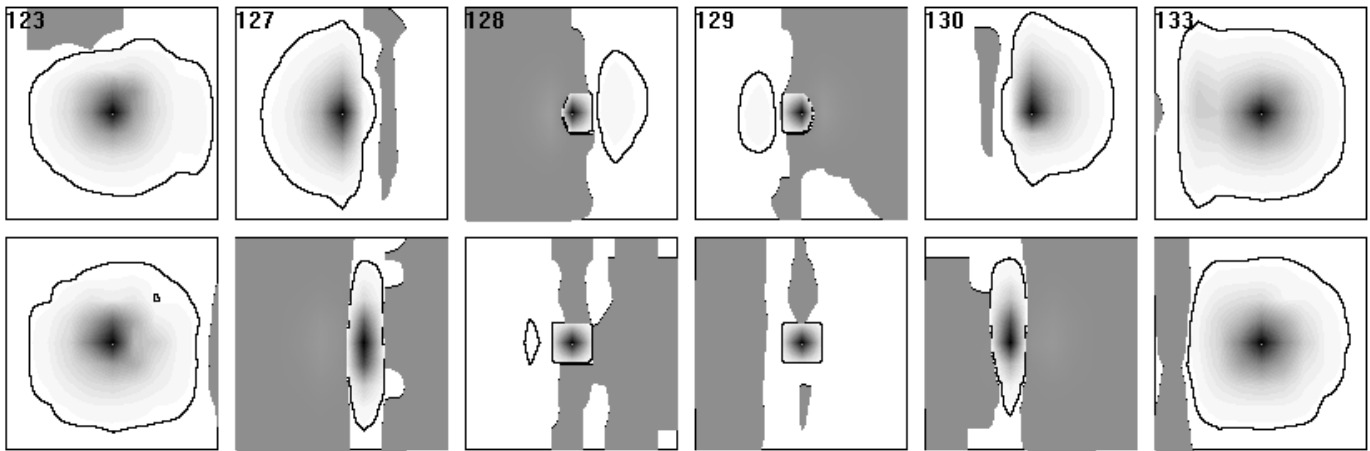
is almost arbitrary and the PL method fails. This means that some boundaries of critical contrast can be corrupted.

Fig.7. PL method.  $\lambda = 0.8$ .  $\mu = 0.7$ .  $y_0 = 27$ 

*GR method.* As show our tests, good convergence is obtained for  $\lambda = 0.8..0.95$ . Thus in the following examples we use the value  $\lambda = 0.85$ . Choosing another  $\lambda$  somewhat changes shape and size of influence areas. However, these changes are not considerable. On the contrary, the choice of the second parameter  $\mu$  is very essential for GR method. Next we show pictures for  $\mu = 0.2$ ,  $\mu = 0.7$ , and  $\mu = 1.0$ .

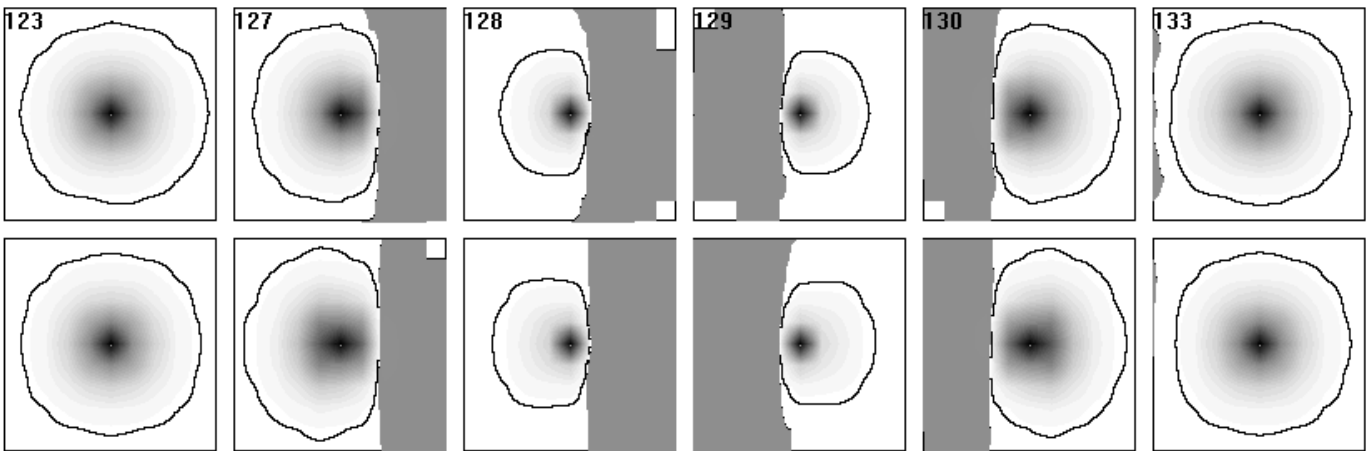
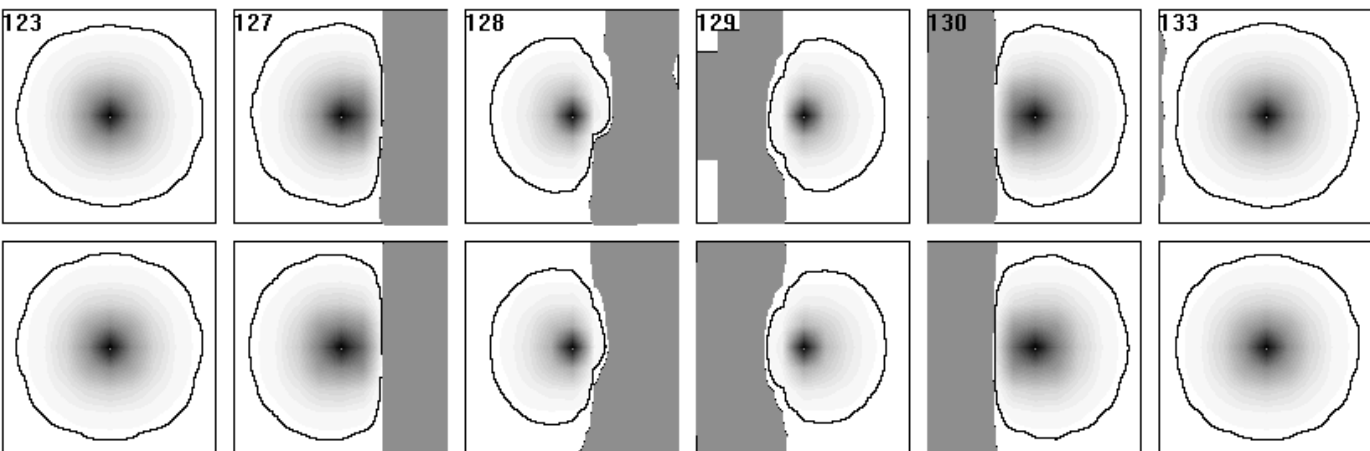
Within the images on Fig.8-10, there are big homogenous gray domains outside  $(x_0, y_0)$  where the function D is less

than zero (both in the first and the second row). It means presence of distortions on the restored image. The distortions are most considerable when  $\mu$  is small ( $\mu = 0.2$ ) on Fig.8). Note that if the tested pixel is close to the boundary ( $x_0 = 128, 129$ ), influence areas are very small. It means that the preserving of contrast boundary is good. So, in the case of small  $\mu$ , GR method has a special feature. It rather distorts the areas with slowly varying intensity than boundaries.

Fig.8. GR method.  $\lambda = 0.85$ .  $\mu = 0.2$ .  $y_0 = 27$ 

Typical influence areas for  $\lambda = 0.85$ ,  $\mu = 0.3..1.0$  are shown on Fig.9,10. If a pixel is relatively far from the boundary ( $x_0 = 123$  and  $x_0 = 133$ ), influence areas are large. Hence, initial image is blurred in the neighborhoods of such points. Due to this we have noise reduction effect. Most characteristic are images with  $x_0 = 128$  and  $x_0 = 129$ .

However, for greater values of  $\mu$ , the size of influence areas increases near the boundary (see below, Fig.9,10). It means that for such  $\mu$ , the GR method blurs even the most contrast boundaries.

Fig.9. GR method.  $\lambda = 0.85$ .  $\mu = 0.7$ .  $y_0 = 27$ Fig.10. GR method.  $\lambda = 0.85$ .  $\mu = 1.0$ .  $y_0 = 27$

## VI. CONCLUSION

As seen from the above, the influence areas play the key role in the novel technique for testing of energy minimizing restoration methods. We used this technique for calculation of these areas and applied the whole testing procedure to a couple of restoration methods: PL and GR. We studied their ability to simultaneously reduce the noise and to preserve contrast boundaries on the restored image. In our testing procedure, the evaluated method is considered as a black box with input parameters which control its performance.

Our tests showed that for both of the methods there are critical contrast values, which may lead to distorted boundaries of objects on the restored image.

For the PL method, the optimal values of its input parameter  $\lambda$  are in the range from 0.8 to 0.9 and  $\mu$  are from 0.2 to 0.8. For the smaller  $\mu$ , the distortions on the restored images may be observed; bigger values of  $\mu$  often lead to the loss of high contrast boundaries.

The GR method almost always creates distortions on the restored image. Increasing the intensity value at a certain pixel of input image, one may get the decrease of intensity on the restored image. However, this is not a disadvantage of the method, because this effect can increase the contrast of blurred object's boundaries, or in other words, it can increase the image's sharpness. According to our test results, the optimal values of  $\lambda$  for the GR method lay in the range from 0.8 to 0.95. For the high contrast preservation of the object boundaries, the optimal values of  $\mu$  are from 0.1 to 0.2. If noise suppression is the main priority, one should take  $\mu$  from 0.3 to 1.0.

Since the energy minimizing methods are also used for image segmentation (see e. g. [2]-[3], [11]) the considered testing method can be applied to study the segmentation of blurred images by such methods. However, in the results presented here, only step-type boundaries were considered (Fig. 2). So the comprehensive testing of boundary preservation property by such methods remains an open task. We believe that the images from the database of PICASSO system [15]-[16], [20]-[21] can form a representative set for such testing.

## REFERENCES

- [1] M. Wirth, M. Fraschini, M. Masek, M. Bruynooghe: Performance evaluation in image processing (Editorial). *EURASIP Journal in Applied Image Processing*, Volume 2006, article ID 45742, pp. 1-3.
- [2] I.V.Gribkov, P.P.Koltsov, N.V.Kotovich, A.A.Kravchenko, A.S.Kutsaev, A.V.Zakharov: Comparative Study of Image Segmentation Algorithms, Proceedings of the 8-th WSEAS International Conference SSIP 08, Santander, Spain, 2008, pp. 21-28.
- [3] I.V.Gribkov, P.P.Koltsov, N.V.Kotovich, A.A.Kravchenko, A.S.Kutsaev, A.V.Zakharov: Testing of Image Segmentation Methods. *WSEAS Proceedings in Image Processing*, v. 4, No. 8, pp. 494-503, 2008.
- [4] D.Mumford and J.Shah: Boundary detection by minimizing functionals. In *Proc. IEEE Conf. Computer Vision and Pattern Recognition*, San Francisco, CA, 1985
- [5] D.Mumford and J.Shah: Optimal approximations by piecewise smooth functions and associated variational problems. *Commun. Pure Appl. Math.*, v. XLII, pp. 577-685, 1989.
- [6] S.Geman and D.Geman: Stochastic relaxation, Gibbs distributions, and Bayesian restoration of images. *IEEE TPAMI*, v. PAMI-6, pp. 721-741, 1984.
- [7] D.Geman, S.Geman, C.Graffigne, and P.Dong: Boundary detection by constrained optimization. *IEEE TPAMI*, v. 12, pp. 609-628, 1990.
- [8] D.Geman and G.Reynolds: Constrained restoration and the recovery of discontinuities. *IEEE TPAMI*, v. 14, pp. 376-383, Mar. 1992.
- [9] V.Torre and T.Poggio: On edge detection. *M.I.T. Artificial Intell. Lab., Cambridge, MA, Rep. AIM-768*, August 1984.
- [10] T.Poggio, H.Voorhees and A.Yuille: A regularized solution to edge detection. *M.I.T. Artificial Intell. Lab., Cambridge, MA, Rep. AIM-833*, May 1985.
- [11] G.A.Hewer, C.Kenney, and B.S.Manjunath: Variational Image Segmentation Using Boundary Functions. *IEEE Trans. Image Processing*, v.7, No. 9, 1998, pp.1269-1282
- [12] C.Samson, L.Blanc-Feraud, G.Aubert, and J.Zerubia: A Variational Model for Image Classification and Restoration. *IEEE TPAMI*, v.22, No. 5, pp. 460-472
- [13] Y.Boykov, V.Kolmogorov: An Experimental Comparison of Min-Cut/Max-Flow Algorithms for Energy Minimization in Vision. *EMMVCVPR 2001*, pp. 359-374
- [14] O.Veksler: Efficient Graph-Based Energy Minimization Methods in Computer Vision. PhD thesis, Cornell University, July 1999
- [15] I.V.Gribkov, P.P.Koltsov, N.V.Kotovich, A.A.Kravchenko, A.S.Kutsaev, A.V.Zakharov: PICASSO 2- a System for Performance Evaluation of Image Processing Methods, Proceedings of the 5th WSEAS Int. Conf. on Signal Processing, Computational Geometry and Artificial Vision, Malta, September 15-17, 2005, pp. 88-93.
- [16] I.V.Gribkov, P.P.Koltsov, N.V.Kotovich, A.A.Kravchenko, A.S.Kutsaev, A.V.Zakharov: Empirical evaluation of Image Processing Methods Using PICASSO 2 System, *WSEAS Transactions on Systems*, v. 4, No 11, 2005, pp. 1923-1930.
- [17] V.Torre and T.Poggio: On Edge Detection. *M.I.T. Artificial Intell. Lab., Cambridge, MA, Rep. AIM-768*, 1984.
- [18] P.Courtney and N.A.Thacker: Performance Characterisation in Computer Vision: The Role of Statistics in Testing and Design. In *Imaging and Vision Systems: Theory, Assessment and Applications*, J. Blanc-Talon and D. Popescu (Eds.), NOVA Science Books, 2001.
- [19] K.W.Bowyer and P.J.Phillips: Overview of Work in Empirical Evaluation of Computer Vision Algorithms. In *Empirical Evaluation Techniques in Computer Vision*, K.W. Bowyer and P.J. Phillips (Eds.), IEEE Computer Press, 1998.
- [20] I.V.Gribkov, P.P.Koltsov, N.V.Kotovich, A.A.Kravchenko, A.S.Kutsaev, V.K.Nikolaev, A.V.Zakharov: PICASSO - Edge Detectors Evaluation System Based on the Comprehensive Set of Artificial Images, Proceedings of the 6th World Multiconference on Systemics, Cybernetics and Informatics, Vol. 9, 2002, pp 88-93.
- [21] I.V. Gribkov, P.P. Koltsov, N.V. Kotovich, A.A. Kravchenko, A.S. KoutsaeV, V.K. Nikolaev, A.V. Zakharov, Testing of Energy Minimizing Methods in Image Preprocessing Using the PICASSO System, Proceedings of the 8th World Multiconference on Systemics, Cybernetics and Informatics, Vol. 6, 2004, pp 233-238.
- [22] M. Kitchener, A. Bouzerdoum & S. Phung: Adaptive regularization for image restoration using a variational inequality approach. *IEEE 17th International Conference on Image Processing*, 2010, pp. 2513-2516.
- [23] A. Alfiansyah: Colour Image Restoration via Total Variation Regularization. *Jurnal TEKNOIN*, vol 15, no 1, September 2010. Faculty of Industrial Engineering, Islamic University of Indonesia.
- [24] Babacan, S.D., Molina, R., Katsaggelos, A.K.: Sparse Bayesian image restoration. *17th IEEE International Conference on Image Processing (ICIP)*, 2010, 26-29 Sept. 2010, pp. 3577 – 3580.
- [25] Michael K. Ng, Andy C. Yau: Super-Resolution Image Restoration from Blurred Low-Resolution Images. *Journal of Mathematical Imaging and Vision - JMIV*, 2005, vol. 23, no. 3, pp. 367-378.
- [26] Mingjun Wang, Shuxian Deng: Image Restoration Model of PDE Variation. *Second International Conference on Information and Computing Science*, 2009. ICIC '09. 21-22 May 2009 pp. 184 – 187.